

Research on Unsteady Plasma Plume by DSMC/PIC Hybrid Algorithms

Jie Li, Yongyuan Su, Zhenglei Fan, Jiawei Ye

National University of Defense Technology, College of Aerospace Science and Engineering,

Changsha 410073, China

Lijie_gfd@163.com

Abstract

Based on the in-house DSMC program and PIC program, the Fortran/C++ mixed-language programming is used to implement the DSMC/PIC hybrid algorithm. In the PIC module, the electric field is solved by Poisson equation. In the DSMC module, the chemical combination and dissociation of the neutral particles is numerically simulated. The DSMC/PIC hybrid algorithm is employed in the process of the injection of the atomic hydrogen H and ion H⁺ into a vacuum cylinder through the bottom surface. Results have shown that the region of the diffusion of ion H⁺ is larger than that of atomic hydrogen H, and the diffusion speed is even faster than that of atomic hydrogen H.

1. Introduction

Plasma plume is widely used in the fields of industrial coatings^[1], nuclear fusion reactor^[2], and plasma thrusters^[3], such as micro-cathode vacuum arc thrusters^{[4] [5]}. In these devices, where plasma arc jets flow, the dimensions are sometimes very small and this results in the flow field being not a continuum, and the plasma jet is very rarefied, so it is often called plasma plume. In the plasma plume induced by the pulsed vacuum arc, the coupling characteristics of flow field and electric field are significant. The motion of charged ions forms a self-consistent electric field so that the motion of charged ions is more complicated in the self-consistent electric field and the additional electric field. The temporal and spatial distribution and evolution characteristics of particles in the flow field are seriously affected by the electric field. For the pulse vacuum arc plasma plume, direct simulation Monte Carlo method (DSMC) and particle in cell method (PIC) are used to research, specifically neutral particles are tracked using DSMC method and charged ions are tracked using PIC method.

DSMC method is a numerical method developed by Bird^[6] based on Monte Carlo method to simulate physical and chemical processes of particles. Bird^[7] proved the consistency of the numerical solution with DSMC method and the solution with the Boltzmann equation. DSMC method is a physically based probabilistic simulation rather than any common solvers of standard numerical analysis to mathematical equations^[6]. Instead of directly calculating the macroscopic quantities in the flow field, a large number of simulation particles are employed in the flow field. Each simulation particle represents a large number of real particles to simulate the physical and chemical process described by the Boltzmann equation. Pham Van Diep G et al.^[8] used DSMC method to study hypersonic shock wave structure in 1989. The research paper was published in Science, which made DSMC method begin to play an important role in the field of rarefied gas dynamics and was widely used in the engineering fields. With the improvement of DSMC method and the enrichment of complex physical models, DSMC method is gradually used to solve the problems of non-equilibrium thermochemistry^[9], thermal radiation^[10], gas-solid interaction^[11], laser transmission^[12] etc.

PIC method is a numerical simulation method developed by Dawson^[13], Eldridge and Feix^[14] in 1962. After the PIC method was proposed, Hockney et al.^[15] solved the Poisson equation discretely by using the spatial difference method. Since then, PIC method has been widely used in the numerical simulation of electric propulsion plume plasma plume or in the other fields^[16]. After several years of development, PIC method has been successfully applied to the field of plasma and can be used to solve a variety of complex physical problems^{[17] [18]}.

In view of the complicated characteristics of multi-field coupling of plasma plume, a hybrid DSMC/PIC algorithm is proposed to study the spatial and temporal distribution of plasma plume in this paper. Combining the in-house DSMC program with PIC program, the hybrid algorithm is studied and employed in the process of the injection of the atomic hydrogen H and ion H⁺ into a vacuum cylinder through the bottom surface.

2. Implementation of DSMC/PIC hybrid algorithm

Based on the in-house DSMC program and PIC program, the Fortran/C++ mixed-language programming is used to implement the DSMC/PIC hybrid algorithm. The DSMC program and the PIC program are individually written in Fortran and C++ language. On the basis of DSMC module, PIC module is added by the Fortran/C++ mixed-language programming. DSMC module is used to simulate all physical models related to neutral particles, including collisions between neutral particles, neutral particles and charged ions, chemical reactions involving neutral particles, and chemical reactions with the wall. PIC module is mainly used to solve Poisson equation to simulate the electric field, track the movement of charged ions in the electric field, and deal with the collisions between charged ions and electrons.

There are many kinds of components in plasma plume. Neutral particles generally move slowly, and ions move faster in the electric field, but there are not much different from neutral particles. The electron mass is small and the velocity is very fast. So the time step of electrons differs greatly from that of neutral particles and ions. When electrons are simulated in the form of particles, the time for calculation increases sharply. So the electrons would be neglected to simulate in this paper. The plasma in the flow field is electrically neutral, and the neutral particles and ions are numerically simulated in the flow field and the electric field.

According to the procedures of DSMC program and PIC program, the procedure of DSMC/PIC hybrid algorithm is given in Figure 1. Next, the details of the procedure of the hybrid algorithm are introduced as follows.

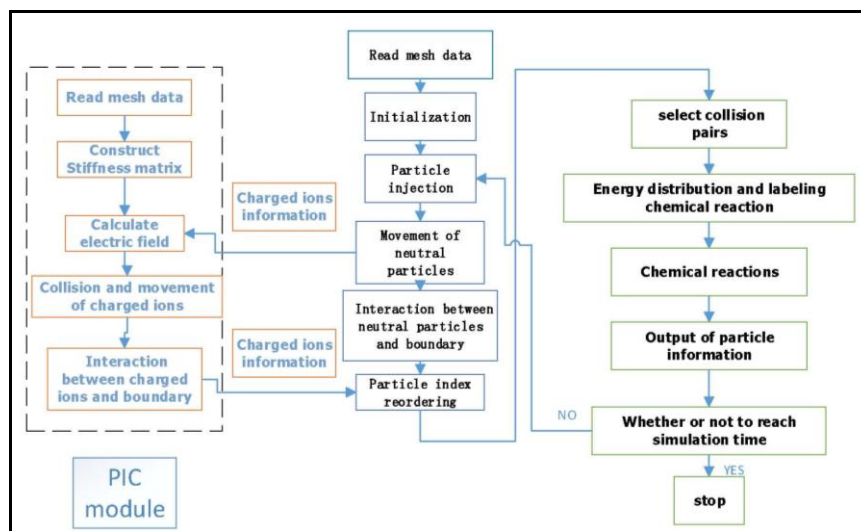


Figure 1: The procedure of DSMC/PIC hybrid algorithms

Firstly, read mesh data. The mesh used in the program is tetrahedral unstructured. The grid is processed by calculating the parameters of the mesh centre, volume and area, and the adjacent grids of each mesh, the number of grids contained in each node are recorded, and the surface mesh on all the boundaries are marked. Then the inner normal direction of each boundary surface is calculated. The different mesh information needed by DSMC and PIC are separately stored in the files after the processing of the mesh information.

Secondly, initialization. The initialization includes in DSMC module and PIC module. The initialization of DSMC module mainly includes defining and storing parameter information about particles. According to the given information of injected particles, weight factor and time step are selected, and collision pair information is calculated based on the type of injected particles. If the initial flow field is non-vacuum, particles will be placed in the background field. The initialization of PIC mainly includes defining and storing parameters about the Poisson equation. The stiffness matrix K for solving Poisson equation is constructed, and the initial potential boundary conditions are given.

Then, injection of particles. Particle injection can be divided into neutral particle injection and ion injection. The density of neutral particles is more than one or two orders of magnitude different from the density of ions, so the time step and the weight factor for neutral particles and ions are different too. Thus the neutral particles and charged ions are injected separately, but all of them are based on the Maxwell distribution at a given velocity. The injecting particles are all marked in order.

Next, particle movement. Particle movement module, as the core module of DSMC/PIC hybrid algorithm, involves data transfer between DSMC and PIC. The data transfer mode is shown in Figure 2. After particle injection, the particle movement is divided into two parts. One is the neutral particle movement, the other is the ion movement. The neutral particle movement is processed by the traditional DSMC method, and the interaction between the neutral

particle and the boundary is processed, including the wall reflection model and the wall chemical reaction model. The information of charged ions is stored in the temporary two-dimensional array DTPIC when all the simulated particle movements are completed. The ion information includes velocities, positions, the mesh number and the global labelling number of the simulated particles. After all the simulated particles move, the data chain DTtoPIC is opened dynamically according to the number of ions at the current time, and all the information of charged ions is stored in the data chain DTtoPIC. The ion information is transmitted to the PIC module, where the data of ion is read directly from the data chain DTtoPIC. The electric field is calculated by solving Poisson equation based on the ion information. The charged ion moves in a time step in the electric field. At the same time, the collision and interaction with the wall between ions, including particle adsorption or reflection on the wall, and the chemical reaction on the wall, are processed. According to the model, the velocity and location information of charged ions are assigned to the data chain DTtoPIC after the ion movement. In the DSMC module, the data chain DTtoPIC is read to obtain the charged ion information, and the global number of the simulated particles is relabelled.

Lastly, after the particle movement, the DSMC/PIC hybrid algorithm is to reorder the particles, select collision pairs, deal with collision and energy distribution between particles, label particles involved in the chemical reactions. The particle information is currently stored in the form of a file for calculating the physical macro-quantities in the post-processing module. If the simulation time is not reached, the particles will continue to be injected, otherwise the programme will be stopped.

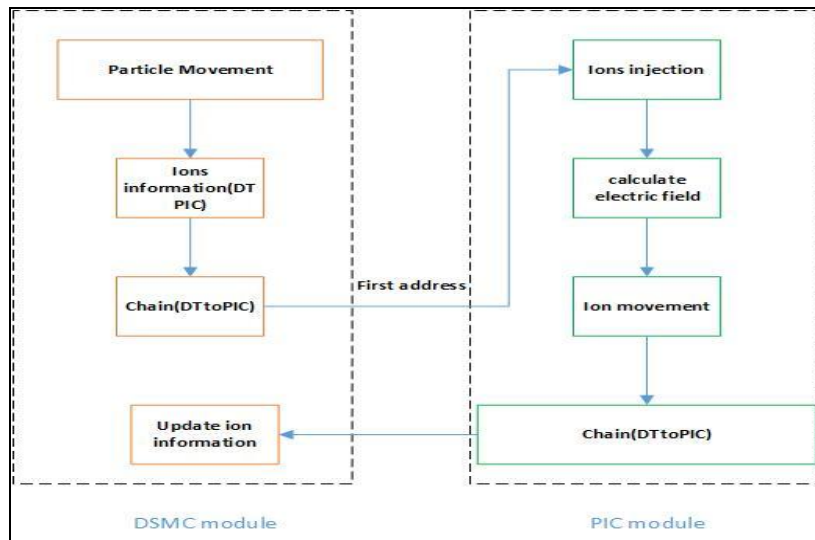


Figure 2: Data transfer in the DSMC/PIC hybrid algorithms

3. Numerical simulation of the unsteady rarefied plasma flows based on the DSMC/PIC method

For the DSMC and PIC methods, the requirements of the grid spatial scales are different. The DSMC method requires the grid spatial scale to be the magnitude of the molecular mean free path, while the PIC method requires it to be the magnitude of the Debye length. In order to meet the grid requirements of the DSMC and PIC method, different number densities of neutral particles and charged ions are considered to ensure that the one set of the grid can meet the requirements of both methods. That is, the average free path of neutral particles and the Debye length of charged ions are in the same order of magnitude.

Figure 3 shows the geometry of the computational domain with length 0.6 m and radius 0.25 m. The particles enter into the field from the inlet with the diameter 0.1m, as shown by the red line. The black lines represent the wall. The temperature of the wall is 300 K, and the diffusion reflection model is used for the gas-surface interactions. The charged particles which reach the left wall will immediately be changed to be neutral particles. While ensuring that the plasma flow field is electrically neutral, it is assumed at the same time when the electrons reach the wall that they disappear, so the potential of the left wall is considered to be zero. The potential of the right wall is -50v as one of the given boundary conditions. The particles are composed of H and H⁺, and the detailed inlet conditions are shown in Table 1. The variable soft sphere (VSS) model and the Larsen-Borgnakke model is used for the binary molecular collisions^[7]. In the simulation, 4216 nodes and 19622 tetrahedral volume elements with local mesh refinements are used for the DSMC/PIC method, and the grid of computational domain is shown in Figure 4.

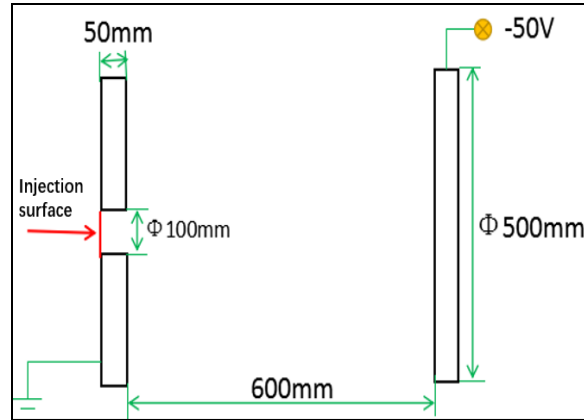


Figure 3: The computational domain

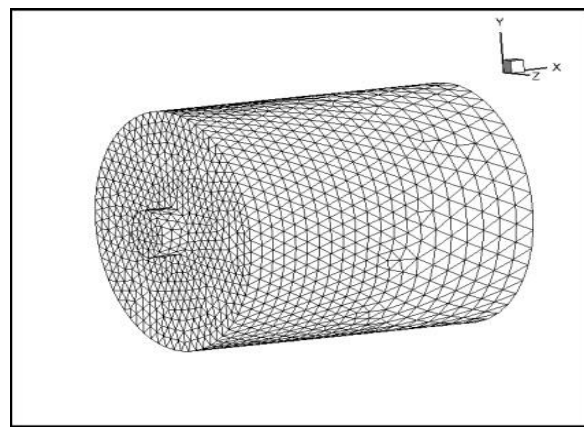


Figure 4: The grids of the computational domain

Table 1: THE INLET CONDITIONS OF THE PARTICLES

Component	Number density (m^{-3})	Velocity (m/s)	Temperature (ev)	Time step (s)	Weigh factor
H	1×10^{20}	1×10^4	0.1	1.0×10^{-7}	5.0×10^{11}
H^+	3×10^{10}	1×10^4	0.5	5.0×10^{-8}	200

Figure 5 shows the density distributions of the atomic hydrogen H and the ion H^+ at different times on the $Z = 0$ plane. The number density distribution of the atomic hydrogen H is basically the same as that calculated by the DSMC programme. The flow field is basically steady at the time around $40\mu\text{s}$, and there is no obvious change after that. There is no atomic hydrogen H in the left corners of the large cylinder, which indicates that atomic hydrogen H does not completely diffuse into the whole space at the time $60\mu\text{s}$. Comparing with the number density distribution of ion H^+ , it can be seen that the number density distribution area of the ion H^+ is larger than that of the atomic hydrogen H at the same time. In the electric field, the velocity of the ion H^+ accelerates, and the ion H^+ movement forms a self-consistent electric field, which hinders the ion H^+ movement. Therefore, the diffusion area of the ion H^+ along the axis is larger, so after the time $30\mu\text{s}$, the low-density area of the ion H^+ appears, but there is still no ion H^+ in the left corners of large cylinder, indicating that the ion H^+ does not diffuse into the whole space within the time $60\mu\text{s}$ and the flow field does not reach steady. Compared with the number density distribution of the atomic hydrogen H and the ion H^+ at the same time, it can be seen that the high density region of the atomic hydrogen H is balloon-shaped, while the high density region of the ion H^+ only appears on the left side of the small cylinder near the injection surface, which indicates that the diffusion rate of the ion H^+ in the electric field is faster than that of the atomic hydrogen H.

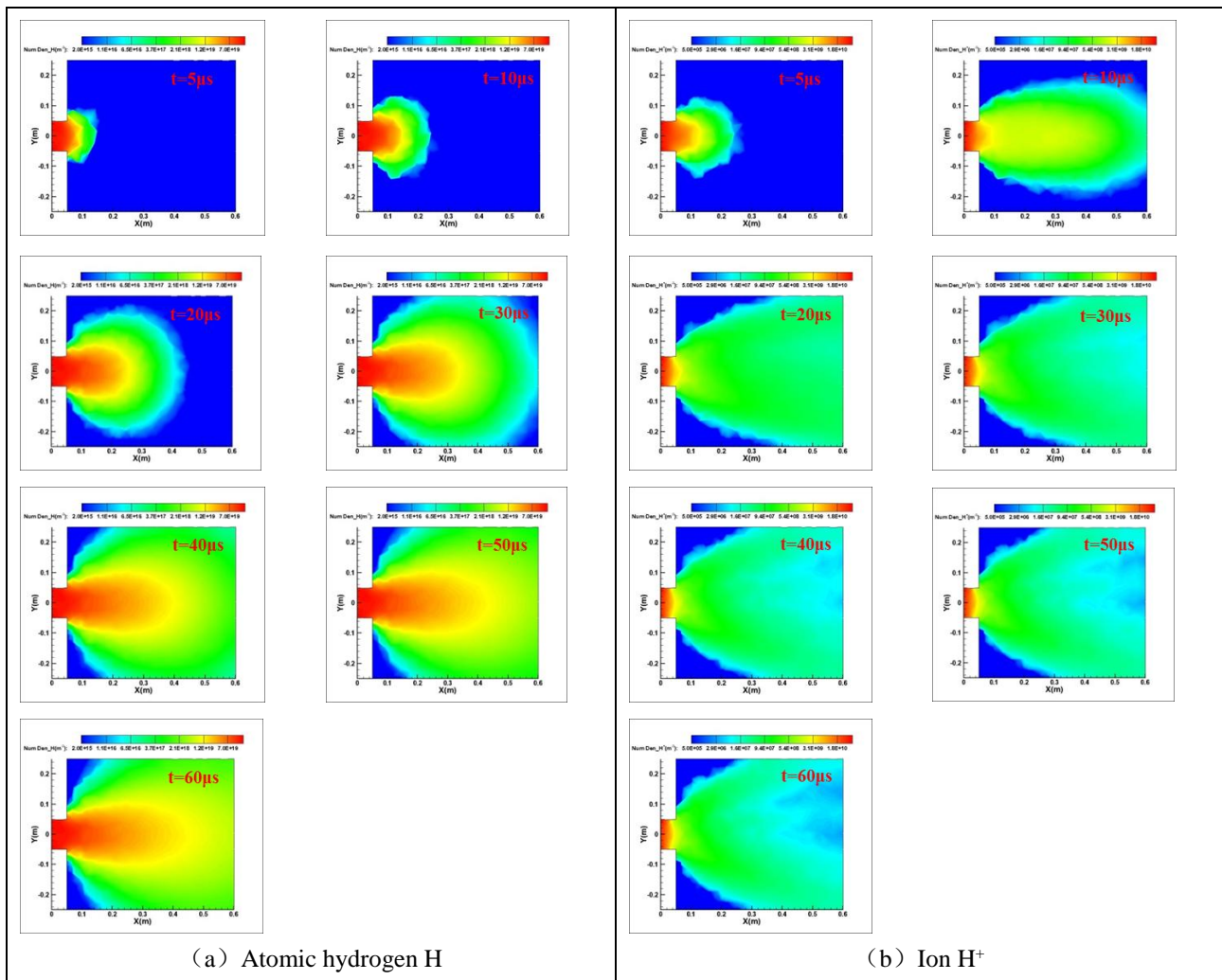
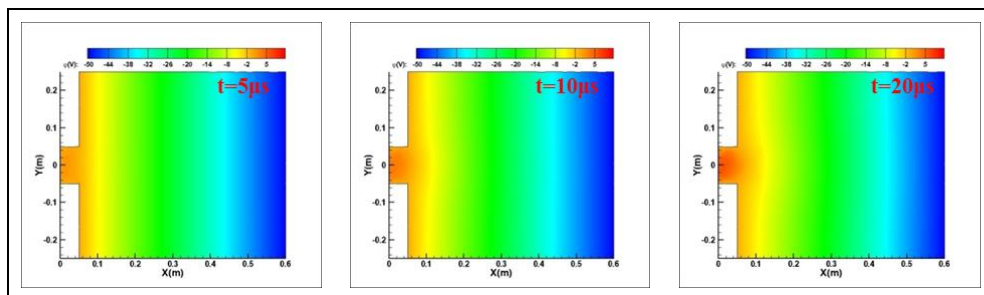


Figure 5: The evolution of the number density of the atomic hydrogen H (left) and the ion H⁺ (right) in the symmetrical plane

Figure 6 shows the electric potential distribution at different times on the $Z = 0$ plane. The electric potential is the highest near the inlet and the lowest near the right wall. Because the boundary condition for the electric potential on the right wall is the Dirichlet boundary condition, the electric potential on the wall is the lowest. The electric potential changes fast in the vicinity of $X=0.1\text{m}$ and $X=0.42\text{m}$, because the boundary of the left metal surface and the right metal wall are the Dirichlet boundary conditions. For the elliptic partial differential equations such as Poisson equation, the Dirichlet boundary has a great influence on the results. With the increase of the time, the electric potential near the inlet will gradually increase until it reaches the stable value. Because the ion H⁺ is injected into the flow field, the ions gather near the inlet, resulting in a gradual increase of the electric potential near the inlet until it reaches a stable value.



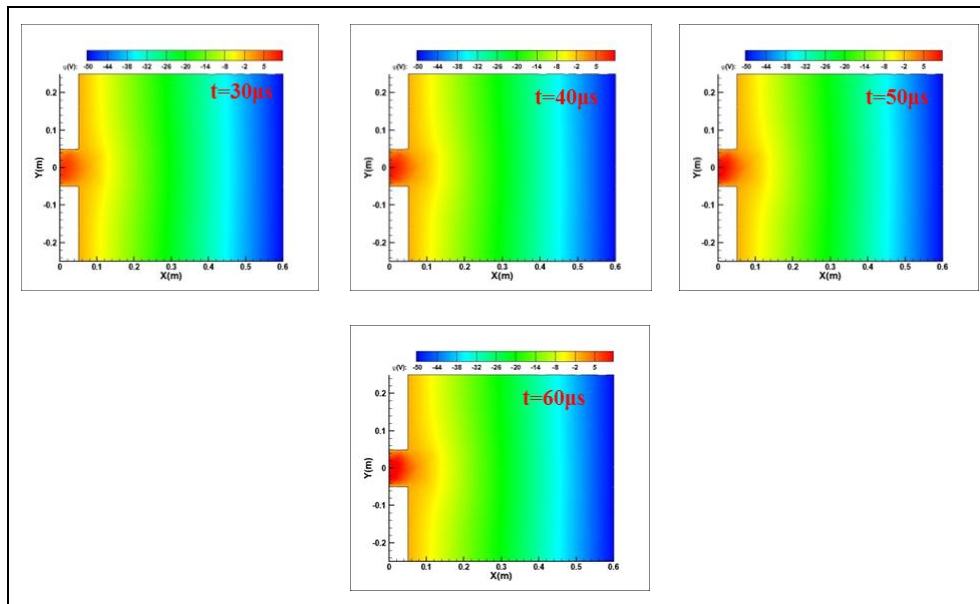


Figure 6: The evolution of the electric potential distribution in the symmetrical plane

Figure 7 shows the electric potential along the symmetric axis at different times. The electric potential near the inlet is positive, and it decreases gradually along the X direction. After $X = 0.05\text{m}$, the electric potential changes linearly. On the right wall boundary, the electric potential is given -50V , as Dirichlet boundary condition. With the increase of time, the overall potential increases gradually, but the increasing trend is less obviously, and finally the electric field tends to be steady. With the increase of the distance along the X direction, the electric potential gradually decreases.

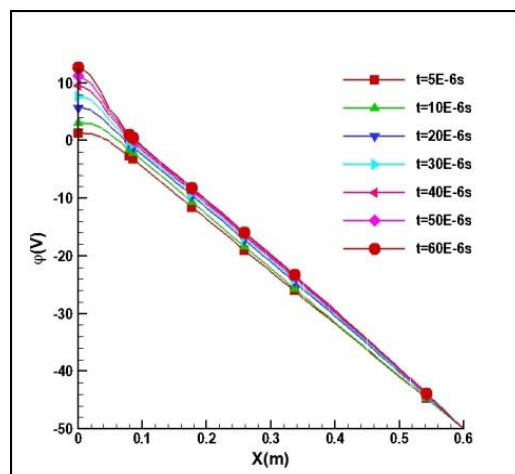


Figure 7: The electric potential along the symmetric axis at different times

Figure 8 shows the number density of the atomic hydrogen H and the ion H^+ along the axis at different times on the symmetric axis. The atomic hydrogen H does not reach the right end before the time $30\mu\text{s}$. The number density of the atomic hydrogen H decreases rapidly to zero. As the time goes on, the number density of the atomic hydrogen H gradually diffuses along the X direction and increases gradually with the time. After the time $30\mu\text{s}$, the atomic hydrogen H moves to the right end. Then the number density of the atomic hydrogen H at the same position increases gradually until it reaches the stable value. According to the number density of the ion H^+ , the ion H^+ does not move to the right end at the time $5\mu\text{s}$, and the number density decreases rapidly to zero. At the time $10\mu\text{s}$, the ion H^+ has diffused to the right end. But at this time, the number density of the ion H^+ drops rapidly along the X direction, then decreases slowly, and finally decreases rapidly. As the time increases, the number density of the ion H^+ at the same position decreases gradually until it reaches the stable value. Compared with the number density of the atomic hydrogen H along X direction, the number density of the ion H^+ decreases rapidly near the inlet surface, and then gradually becomes steady. The change of the number density of the ion H^+ with time is opposite to that of the atomic hydrogen H. The number density of the atomic hydrogen H increases to be steady with time, and the number density

of the ion H^+ decreases to be steady. This indicates that the ion H^+ diffuses fast in the electric field, and the number density of ion H^+ decreases gradually.

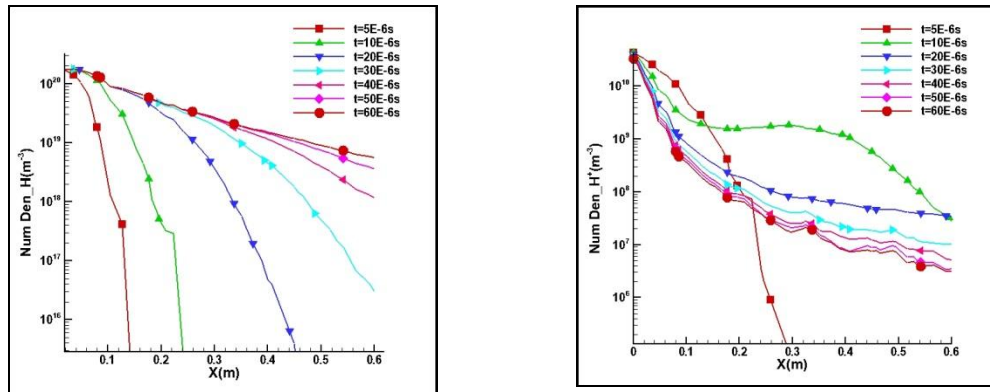


Figure 8: The number density of the atomic hydrogen H (left) and the ion H^+ (right) along the axis

Fig. 9 shows the temperature of the atomic hydrogen H and the ion H^+ along the X direction at different times on the symmetric axis. The temperature of the atomic hydrogen H drops rapidly to zero when the atomic hydrogen H does not move to the right end surface. When the atomic hydrogen H moves to the right end surface, the temperature rises gradually. This indicates that the thermal kinetic velocity of the atomic hydrogen H increases with the time at the same position, leading to the increase of the translation temperature until it reaches a stable value. The temperature of the ion H^+ decreases rapidly to zero at the initial time and gradually decreases with the time until it reaches the stable value. This indicates that the thermal kinetic velocity of the ion H^+ decreases gradually along the X direction. In the electric field, the ion H^+ diffuses faster than the atomic hydrogen H, and the temperature of the ion H^+ reaches a stable state faster than that of the atomic hydrogen H.

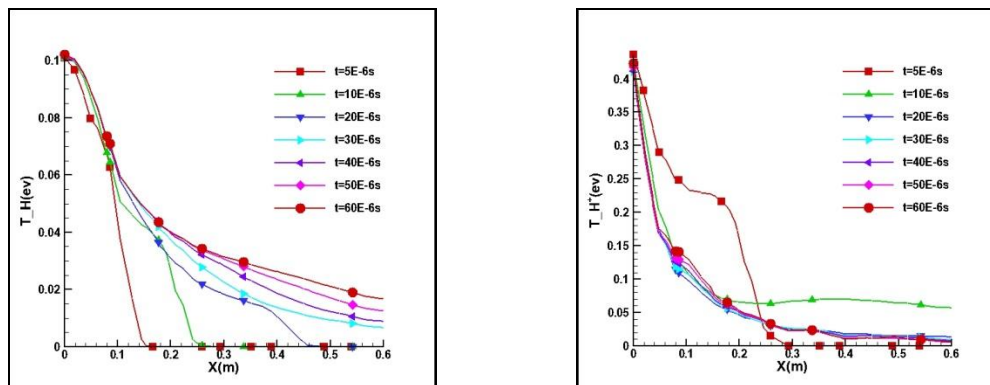


Figure 9: The temperature of the atomic hydrogen H (left) and the ion H^+ (right) along the axis

Figure 10 shows the number density of the atomic hydrogen H and the ion H^+ along the Y direction on a specific line with $X=0.2m$. The number density of the atomic hydrogen H and the ion H^+ rises first and then decreases along the Y direction at the same time, the distribution is basically symmetrical about $Y=0$. When the time is $5\mu s$, the atomic hydrogen H has not diffused to the specific line, but the ion H^+ has diffused to the specific line, which indicates that the ion H^+ diffuses faster than the atomic hydrogen H in the electric field. With the increase of time, the number density of the atomic hydrogen H at the same position gradually increases to the stable value, the number density increases slowly near the symmetric axis, and the number density increases rapidly near the two ends of the specific line. The number density of the ion H^+ increases firstly, then decreases gradually to the stable value near the symmetrical axis. The number density of the ion H^+ increases gradually to the stable value near the two sides of the specific line. At the time $5\mu s$, the ion H^+ has spread to the vicinity of the specific line, but it has not fully diffused along the Y direction. After the time $10\mu s$, the ion H^+ has fully diffused in the vicinity of the specific line.

Figure 11 shows the temperature of the atomic hydrogen H and the ion H^+ along Y direction on the specific line with $X=0.2m$. The changes of the temperature of the atomic hydrogen H and the ion H^+ along Y direction are basically the same. They all increase gradually at first, then decrease, and reach the maximum near the symmetric

axis. The temperature of the atomic hydrogen H gradually increases to the stable value, while the temperature of the ion H^+ gradually decreases to the stable value near the symmetric axis. The temperature of ion H^+ increases gradually to the stable value on both sides of the specific line. The results show that the thermal kinetic velocity of the ion H^+ gradually decreases near the symmetric axis, with the increase of the time, the flow field tends to be steady gradually, and the thermal kinetic velocity decreases. In the diffusion movement, the ion motion is mainly affected by the electric field, and the thermal kinetic velocity increases gradually.

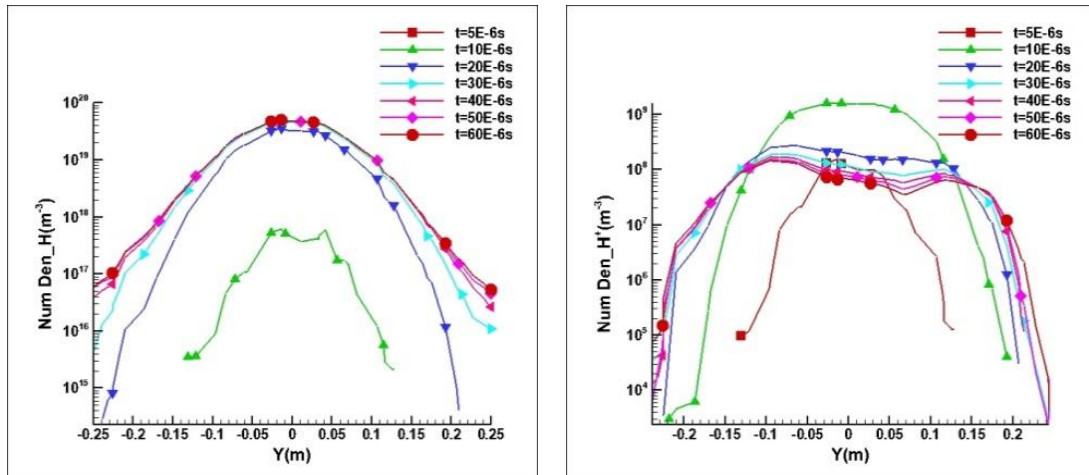


Figure 10: The number density of the atomic hydrogen H (left) and the ion H^+ (right) along the line of $x=0.2m$

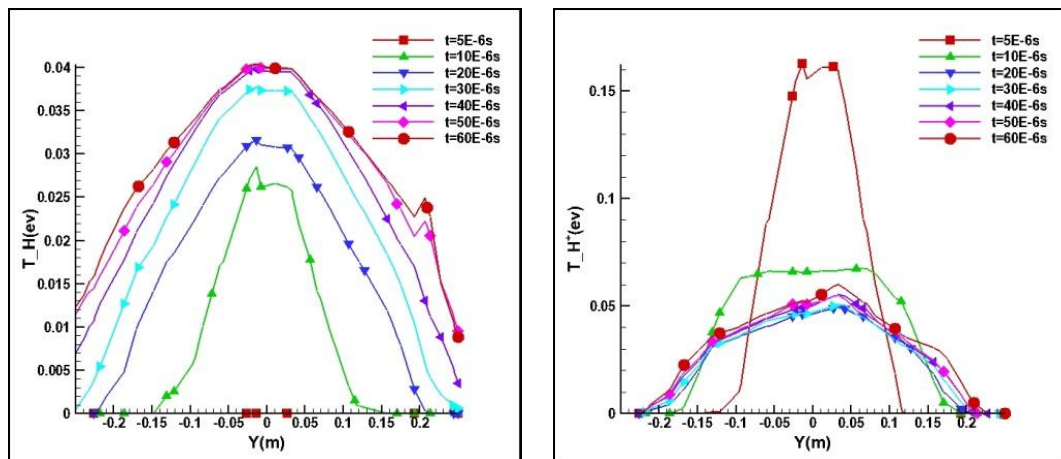


Figure 11: The temperature of the atomic hydrogen H (left) and the ion H^+ (right) along the line of $x=0.2m$

3. SUMMARY

In the current study, the DSMC/PIC hybrid algorithms based on the Fortran/C++ mixed-language in-house code are employed to investigate numerically the unsteady plasma plume. In the PIC module, the electric field is solved by Poisson equation, and the double weight factor and double time step are used in a set of grids, which enable the numerical simulation of charged ions and neutral particles. In the DSMC module, the chemical combination and dissociation of the neutral particles is numerically simulated. The DSMC/PIC hybrid algorithm is employed in the process of the injection of the atomic hydrogen H and ion H^+ into a vacuum cylinder through the bottom surface. Results have shown that the region of the diffusion of ion H^+ is larger than that of atomic hydrogen H, and the diffusion speed is even faster than that of atomic hydrogen H. Along the symmetry axis, the number density and the temperature of atomic hydrogen H and ion H^+ have gradually decreased. The difference is just that the number density of atomic hydrogen H increases with time, while ion H^+ decreases with time. Along the line of $X=0.2m$, the density and the temperature of atomic hydrogen H and ion H^+ are basically symmetrical about the line of $Y=0$, and accordingly, the density of the atom H increases with time, but the ion H^+ increases firstly and then decreases with time.

Acknowledgements

The authors would like to express their thanks for the support from the National Natural Science Foundation of China and NSAF (Grant No.U1730247).

References

- [1] Hirata Y, Kato T, Choi J. DLC Coating on a Trench-Shaped Target by Bipolar PBII [J]. *International Journal of Refractory Metals & Hard Materials*, 2015, 49(1): 392~399.
- [2] Francesco, Taccogna, Pierpaolo, et al. Kinetic Divertor Modeling [J]. *Chemical Physics*, 2012, 398(1): 27~32.
- [3] Korkut B, Li Z, Levin D A. 3-D Simulation of Ion Thruster Plumes Using Octree Adaptive Mesh Refinement [J]. *IEEE Transactions on Plasma Science*, 2015, 43(5): 1706~1721.
- [4] Zhuang T S, Shashurin A, Haque S, et al. Performance Characterization of the Micro-Cathode Arc Thruster and Propulsion System for Space Applications [J]. *Breastfeeding Medicine the Official Journal of the Academy of Breastfeeding Medicine*, 2013, 7(5): 337~442.
- [5] Choueiri E Y. Plasma Oscillations in Hall Thrusters [J]. *Physics of Plasmas*, 2001, 8(4): 1411~1426.
- [6] Bird G A. *Molecular Gas Dynamics* [M]. Clarendon Press, Oxford, 1976: 166~186.
- [7] Bird G A. Direct Simulation of the Boltzmann Equation [J]. *Phys. Fluids*, 1970, 13 (13):2676~2681.
- [8] Phamvandiep G, Erwin D, Muntz E P. Non-equilibrium Molecular Motion in a Hypersonic Shock Wave [J]. *Science*, 1989, 245(4918):624.
- [9] Boyd I D. Rotational and Vibrational Non-equilibrium Effects in Rarefied Hypersonic Flows [J]. *Journal of Thermophysics and Heat Transfer*, 1990, 4(4): 478~484.
- [10] Everson J, Nelson H F. Development and Application of a Reverse Monte Carlo Radiative Transfer Code for Rocket Plume Base Heating [R]. 1993, AIAA Paper 93~138.
- [11] Plastinin Y, Anfimov N, Baula G, et al. Modeling of Aluminum Oxide Particle Radiation in a Solid Propellant Motor Exhaust [R]. AIAA paper, 96~1897.
- [12] Wang Hongxia, Liu Daizhi, Song Zibiao, et al. Monte Carlo Simulation of Laser Transmission Through a Smoke Screen [J]. *Chinese Journal of Computational Physics*, 2013, 30(3):415~421.
- [13] Dawson J. One-Dimension Plasma Model [J]. *Phys. Fluids*, 1962, 5:445.
- [14] Eldridge O C, Feix M. One-Dimensional Plasma Model at Thermodynamic Equilibrium [J]. *Mathematical Physics in One Dimension*, 1962, 5(9):103~107.
- [15] Hockney R W. A fast Direct Solution of Poisson's Equation Using Fourier Analysis [J]. *J.assoc.comput.mach.*, 1965, 12(1):95~113.
- [16] Langdon A B, Birdsall C K. Theory of Plasma Simulation Using Finite - Size Particles [J]. *Physics of Fluids*, 1970, 13(8):2115~2122.
- [17] Buneman O. Dissipation of Currents in Ionized Media [J]. *Physical Review*, 2008, 115(3):503~517.
- [18] Zhou J, Liu D, Liao C, et al. CHIPIC: An Efficient Code for Electromagnetic PIC Modeling and Simulation [J]. *IEEE Transactions on Plasma Science*, 2009, 37(10):2002~2011.